HHS Public Access

Author manuscript

Cell Calcium. Author manuscript; available in PMC 2017 April 01.

Published in final edited form as:

Cell Calcium. 2016 April ; 59(4): 189–197. doi:10.1016/j.ceca.2016.02.007.

Male infertility in mice lacking the store-operated Ca^{2+} channel Orai1

Felicity M. Davis[1,*], **Eugenia H. Goulding**[2], **Diane M. D'Agostin**[1], **Kyathanahalli S. Janardhan**[3], **Connie A. Cummings**[4], **Gary S. Bird**[1], **Edward M. Eddy**[2], and **James W. Putney**[1,‡]

[1]Signal Transduction Laboratory, National Institute of Environmental Health Sciences, National Institutes of Health, Research Triangle Park, NC, 27709, USA

[2]Reproductive and Developmental Biology Laboratory, National Institute of Environmental Health Sciences, National Institutes of Health, Research Triangle Park, NC, 27709, USA

[3]Integrated Laboratory Systems, Inc., Research Triangle Park, North Carolina, 27709, USA

[4]UltraPath Imaging, Research Triangle Park, North Carolina, 27709, USA

Abstract

Store-operated calcium entry (SOCE) is an important Ca^{2+} influx pathway in somatic cells. In addition to maintaining endoplasmic reticulum (ER) Ca^{2+} stores, Ca^{2+} entry through store-operated channels regulates essential signaling pathways in numerous cell types. Patients with mutations in the store-operated channel subunit *ORAI1* exhibit defects in store-operated Ca^{2+} influx, along with severe immunodeficiency, congenital myopathy and ectodermal dysplasia. However, little is known about the functional role of ORAI1 in germ cells and reproductive function in mice, or in men, since men with loss-of-function or null mutations in *ORAI1* rarely survive to reproductive age. In this study, we investigated the role of ORAI1 in male reproductive function. We reveal that *Orai1*$^{-/-}$ male mice are sterile and have severe defects in spermatogenesis, with prominent deficiencies in mid- to late-stage elongating spermatid development. These studies establish an essential *in vivo* role for store-operated ORAI1 channels in male reproductive function and identify these channels as potential non-steroidal regulators of male fertility.

Graphical abstract

‡Author for correspondence (putney@niehs.nih.gov).
*Current address: Department of Pathology, University of Cambridge, Cambridge, CB2 1QP, UK

COMPETING INTERESTS

The authors declare no competing financial interests

AUTHOR CONTRIBUTIONS

FMD, EHG, DDA and GSB performed experiments and/or carried out data analysis. FMD, EHG, EME, JWP conceived the study and designed experiments. CAC performed the ultrastructural evaluation. KJ performed the histopathological evaluation of samples. FMD and JWP wrote the main manuscript, and parts were contributed by KJ, CAC and GSB. All authors have approved the final version of the manuscript.

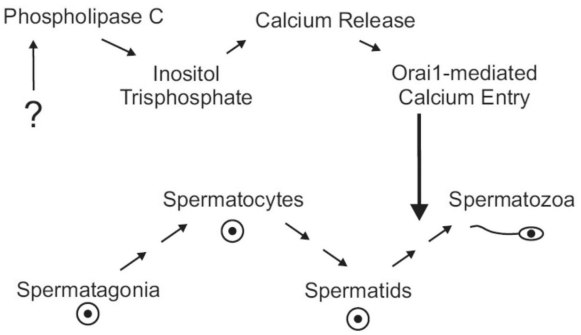

Keywords

Ca^{2+}; Orai1; store-operated calcium entry (SOCE); reproduction; fertility; spermatogenesis

1. INTRODUCTION

Calcium signaling is essential for mammalian male reproduction [1;2]. In male gametes, Ca^{2+} signals orchestrate the major structural and functional alterations that are required for sperm to navigate the female reproductive tract and fuse with mature oocytes [2]. The most extensively studied Ca^{2+} channels in mammalian sperm are CATSPER channels. These sperm-specific Ca^{2+} channels are composed of four pore-forming subunits (CATSPER1–4) arranged in a heteromeric complex with three auxiliary subunits (CATSPERβ, γ and δ) [3]. Male mice with a targeted disruption to any of the *Catsper1–4* or *δ* genes are sterile, despite normal germ cell divisions and maturation in the seminiferous tubules of the testes [3]. Analyses of sperm from these animals and from male patients known to have inactivating mutations to *CATSPER1* and *2* [4–6] have revealed that these channels are indispensable for hyperactivated motility (a high-amplitude, asymmetric flagellar beat pattern) in ejaculated sperm. Similarly, sperm from mice with a null mutation to the plasma membrane Ca^{2+} ATPase 4 (*Pmca4*) gene also fail to undergo hyperactivation and display signs of Ca^{2+} overload in their flagella [7]. These studies highlight the importance of Ca^{2+} signaling in male reproductive function, and the delicate balance between Ca^{2+} entry and extrusion mechanisms in the functional competence of ejaculated sperm.

Ca^{2+} signaling is also essential for fertilization and pre-implantation embryo development [8]. However, *Orai1*$^{-/-}$ female mice are fertile [9], consistent with previous *ex vivo* analyses showing that pharmacological inhibition of SOCE is ineffective in blocking sperm-induced egg activation [10]. Here, we investigated the requirement for ORAI1 in male fertility *in vivo*. We demonstrate that *Orai1*$^{-/-}$ male mice are infertile, owing to a defect in spermatid maturation and progressive degeneration and atrophy of the seminiferous tubules of the testes. This study clearly demonstrates that the Ca^{2+} channel subunit ORAI1 is required for male reproductive function in mice, and similar to T cells [11], skeletal muscle [12] and mammary myoepithelial cells [9], ORAI1 is required without redundancy of function in developing male germ cells.

2. MATERIALS AND METHODS

2.1 Reagents

EmbryoMax M-2 culture medium was purchased from Merck Millipore. Bouin's fixative was purchased from Polysciences, Inc. QIAshredder Homogenizer Columns, RNeasy Plus Mini Kits and Omniscript RT Kits were purchased from Qiagen. The following TaqMan Gene Expression Assays were purchased from Applied Biosystems: *Orai1* (Mm00774349_m1), *Orai2* (Mm04214089_s1), *Orai3* (Mm01612888_m1), *Stim1* (Mm01158413_m1) and *Stim2* (Mm01223103_m1). Several antibodies were used in an attempt to quantitate Orai1 protein in mouse tissues, without success. These were: #ACC-062, Alomone Labs, Jerusalem Israel; #4281 and #4041, ProSci Incorporated, Fort Collins, CO; #21001, New East Biosciences, Malvern, PA; #08264, Sigma-Aldrich, St. Louis, MO; #PA1-74181, ThermoFisher Scientific, Durham, NC.

2.2 Animals and procedures

Orai$^{+/-}$ mice were provided by Dr Jean-Pierre Kinet (Harvard Medical School). *Orai1*$^{-/-}$ mice exhibit a high incidence of perinatal lethality, which was improved by further outbreeding to ICR (CD-1) outbred mice (Harlan Laboratories Inc.), maintaining newborn litters on electric heat pads and delaying weaning in potential knockout mice (identified by their small body size), as previously described [13]. Genotyping was performed on tail DNA by PCR [9]. The following primers and reaction conditions were used to distinguish *Orai1*$^{+/+}$ (488 bp), *Orai1*$^{+/-}$ and *Orai1*$^{-/-}$ (300 bp): 5'-TCA CGC TTG CTC TCC TCA TC-3', 5'-TAA GGG CGA CAC GGA AAT G-3' and 5'-AGG TTG TGG ACG TTG CTC AC-3'; cycling for 95°C for 2 min, 35 cycles of 95°C for 30 s, 60°C for 30 s and 72°C for 45 s, followed by 72°C for 10 min.

Fertility of mature adult (12- to 16- week-old) *Orai1*$^{+/+}$ and *Orai1*$^{-/-}$ male mice was determined by rotated matings of each male with four *Orai1*$^{+/+}$ female mice over two months. Female mice were rotated every two weeks and the number of litters was recorded. All animal procedures were reviewed and approved by the National Institute of Environmental Health Sciences (NIEHS) Animal Care and Use Committee. Animals were housed, cared for, and used in compliance with the *Guide for the Care and Use of Laboratory Animals* in an AAALAC-accredited program.

2.3 Sample collection and sperm analyses

Animals were euthanized by carbon dioxide inhalation. Reproductive organs were dissected, trimmed and weighed. Samples were fixed overnight at 4°C in Bouin's fixative for histology. Samples for real-time RT-PCR were immediately frozen in liquid nitrogen. For sperm analyses, the cauda epididymis was collected in phosphate buffered saline (PBS) at room temperature and transferred to pre-warmed M-2 culture medium. Samples were viewed under a stereoscopic microscope and several small incisions were made along the length of the cauda epididymis using microdissection scissors. Sperm were allowed to move into the medium for 10 min at room temperature. Sperm counts were performed with a hemocytometer, and the percentage of motile and progressively motile sperm was evaluated with a computer-assisted sperm analyzer (CASA, Hamilton Thorne Biosciences).

2.4 Real time RT-PCR

Frozen tissues were ground in liquid nitrogen using a mortar and pestle. RNA lysis buffer (Buffer RLT) was added and samples were passed through a QIAshredder homogenizer column. Total RNA was purified using the RNeasy Plus Mini Kit, with gDNA Eliminator columns to remove any contaminating genomic DNA [14]. Reverse transcription was performed using the Omniscript RT Kit and resulting cDNA was amplified with an Applied Biosystems 7500 Fast Real-time RT-PCR machine, using TaqMan Fast Universal PCR Master Mix and TaqMan Gene Expression Assays (guaranteed 100% ± 10% amplification efficiency), with all reaction conditions and reagents constant. Relative quantification was calculated with reference to 18S ribosomal RNA and analyzed using the comparative CT method [15].

2.5 Histology

Tissues were fixed in Bouin's fixative overnight at 4°C. Samples were washed in PBS with gentle agitation and dehydrated through graded ethanol washes (25–70% ethanol). Tissues were embedded in paraffin, sectioned at 5 μm and stained with hematoxylin and eosin (H&E) or Periodic Acid-Schiff (PAS) hematoxylin stain.

2.6 Electron Microscopy

Mice were euthanized by carbon dioxide inhalation and the testes dissected. The testicular capsule was punctured with a 27G needle and immersed in paraformaldehyde (4%). Tissue was trimmed into 1 mm^3 pieces and processed in an automatic Leica Tissue Processor. Following processing, the samples were embedded into EPON 812 resin blocks. Each resin block was trimmed and sectioned (700–800 nm) and stained with toluidine blue (1%) with subsequent examination by light microscopy. Based on the toluidine blue sections, two blocks for each animal were selected for thin sectioning (approx. 70–90 nm or "gold"). The thin sections were placed on 100-mesh copper grids and stained with uranyl acetate and lead citrate. Grids were visualized on an FEI Tecnai G2 12 Bio Twin 120 KV transmission electron microscope.

2.7 Isolation and Characterization of Mouse Testis Cells

A mixed cell preparation of testis cells isolated from *Orai1*$^{+/+}$ and *Orai1*$^{-/-}$ mice was performed by a method modified from [16]. Briefly, testes from 10 week old *Orai1*$^{+/+}$ and *Orai1*$^{-/-}$ mice were stripped of their tunica albuginea and digested with 0.5 mg/mL collagenase type I (Worthington) in Leibovitz medium (L-15; Gibco) at 32°C in a water bath for 15 minutes then washed 3 times with L-15 to remove interstitial cells. The remaining seminiferous tubules were further digested with 0.25 mg/mL Trypsin Type III (Sigma) in L-15 for 15 minutes at 32°C to release cells. Trypsin Inhibitor Type I-S (0.25mg/ml; Sigma) was then added and the cell suspension pelleted by centrifugation at 240g for 3 min at RT and resuspended in L-15. At this stage, the cells were split and either suspended in L-15 medium for flow cytometric analysis or suspended in complete DMEM (supplemented with 10% fetal bovine serum, 2 mM Glutamine and 100 U/ml Pen/Strep) for intracellular calcium measurements.

Isolated mouse testis cells were loaded with Hoechst 33342 to characterize the distribution of cell populations containing 1n, 2n, or 4n copies of DNA by flow cytometry [17]. Briefly, isolated testis cells were suspended in L-15 medium and incubated with 5 μg/ml Hoechst 33342 for 60 mins at 32°C. Subsequently, flow cytometric analysis was carried out using an LSRII flow cytometer equipped with a 405 nm laser and FACSDiVA software (Becton Dickinson Immunocytometry Systems, San Jose, CA). Individual cells were initially gated on a forward-scatter area vs height dot plot to identify single cells. Propidium iodide was used to gate out dead or dying cells. At least 45,000 viable cells were examined per sample. Forward-scatter versus Hoechst Blue (Ex. 405 nm, Em. 440/40) and Hoechst Red (Ex. 405 nm; Em. 605/40) versus Hoechst Blue dot plots were employed to identify and gate the 1n, 2n and 4n cell populations.

2.8 Single Cell Calcium Measurement

In preparation for intracellular calcium measurements, an isolated mixed testis cell preparation was suspended in complete DMEM and plated on Matrigel (BD Biosciences, Bedford, MA, USA) coated 30 mm round coverslips (#1.5). Cells were allowed to attach to the coverslip and maintained in a humidified 95% air, 5% CO2 incubator at 37°C until used. Fluorescence measurements were made with isolated testis cells loaded with the calcium sensitive dye, fura-5F, as described previously [18]. Briefly, cells plated on Matrigel-coated coverslips and mounted in a Teflon chamber were incubated in complete DMEM with 1 μM acetoxymethyl ester of fura-5F (Fura-5F/AM, Setareh Biotech, Eugene OR, USA) at 37°C in the dark for 20 min. For $[Ca^{2+}]_i$ measurements, cells were bathed in HEPES-buffered salt solution (HBSS: NaCl 120; KCl 5.4; Mg_2SO_4 0.8; HEPES 20; $CaCl_2$ 1.8 and glucose 10 mM, with pH 7.4 adjusted by NaOH) at room temperature. Fluorescence images of the cells were recorded and analyzed with a digital fluorescence imaging system (InCyt Im2, Intracellular Imaging Inc., Cincinnati, OH). Fura-5F fluorescence was monitored by alternatively exciting the dye at 340 and 380 nm, and collecting the emission wavelength at 520 nm. Changes in intracellular calcium are expressed as the “Ratio” (in figures) of fura-5F fluorescence due to excitation at 340 nm and 380 nm (F340/F380). Before starting the experiment, regions of interests identifying single cells were created, with 40 to 50 cells monitored per experiment. In all cases, ratio values have been corrected for contributions by autofluorescence, which is measured after treating cells with 10 μM ionomycin and 20 mM $MnCl_2$.

2.9 Statistics

Statistical analysis was performed using GraphPad Prism 6 for Mac. Statistical tests used for each study are indicated in the figure legends.

3. RESULTS

Orai1$^{-/-}$ male mice showed more than 99% loss of *Orai1* message in the testes compared to *Orai1*$^{+/+}$ controls (Fig. 1). No compensatory changes in the expression of *Orai2*, *Orai3*, or the ER Ca^{2+} sensors *Stim1* or *Stim2* were observed in the testes of *Orai1*$^{-/-}$ mice (Fig. 1). *Orai1* and *Stim1* isoforms were expressed at relatively high levels in the adult mouse testes, suggesting that canonical ORAI1/STIM1 signaling is the predominant SOCE pathway in

this tissue. Unfortunately it was not possible to assess ORAI1 protein expression in cells of the mouse seminiferous tubules with immunohistochemistry due to the lack of suitable mouse antibodies; however, ORAI1 protein is expressed in testicular cells of humans [19].

To assess the consequences of *Orai1* deletion on Ca^{2+} signaling, we made a preparation of dispersed testicular cells [16] and characterized this mixed cell population by flow cytometry [17]. Figure 2 shows that testicular cell preparations from 10-week old mice are predominantly 1n, composed of round spermatids and elongating/elongated spermatids, in roughly equal proportions [20]. Although the proportion of 1n cells and the ratio of 1n/2n cells decreased in the knockout testes, these differences were not statistically significant. Store-operated Ca^{2+} entry was assessed in this population by examining sustained rises in cytoplasmic Ca^{2+} in response to the sarcoplasmic-endoplasmic reticulum Ca^{2+}-ATPase inhibitor, thapsigargin [21] (Figure 3). Cells from $Orai1^{-/-}$ testes showed no sustained entry in response to thapsigargin. This can also be seen in the frequency distribution of sustained $[Ca^{2+}]_i$ (Figure 4). While all cells analyzed from $Orai1^{+/+}$ testes exhibited some degree of sustained $[Ca^{2+}]_i$ in response to thapsigargin, the frequency distribution suggests a minor population with a more limited increase. The identity of this population was not investigated further. More importantly, the fact that all $Orai1^{+/+}$ cells but no $Orai1^{-/-}$ cells showed some degree of sustained Ca^{2+} entry indicates that all seminiferous tubule cells, including spermatogenic cells, have store-operated Ca^{2+} entry and that this is completely lost in $Orai1^{-/-}$ mice.

To determine the importance of ORAI1 in male reproductive function we analyzed reproductive fertility in mice lacking ORAI1 protein [22]. $Orai1^{-/-}$ male mice sired no offspring in rotated matings with wildtype females (Table 1), despite evidence of coitus (vaginal plugs). To investigate the cause for infertility in these animals, we evaluated number and motility of cauda epididymal sperm extracted from $Orai1^{+/+}$, $Orai1^{+/-}$ and $Orai1^{-/-}$ mice. Sperm from $Orai1^{-/-}$ mice had severe defects in motility and progressive motility (Fig. 5). However, sperm counts were also markedly reduced in $Orai1^{-/-}$ mice (Fig. 5), suggesting that, unlike CATSPER channels [23], ORAI1 is required at the level of gamete development in the seminiferous tubules of the testes for the production of functional sperm and for the integrity of sperm during maturation in the epididymis. No abnormalities in the number or motility of mature sperm were observed in $Orai1^{+/-}$ mice (Fig. 5). The lack of a partial phenotype in $Orai1^{+/-}$ mice is likely attributable to the presence of stable cytoplasmic bridges and the sharing of gene products between haploid germ cells, as has previously been described [24].

$Orai1^{-/-}$ mice showed a small but significant reduction in testis weights compared to $Orai1^{+/+}$ and $Orai1^{+/-}$ controls (Table 2). Epididymal and seminal vesicle weights also tended to be lower in $Orai1^{-/-}$ animals; however, total body weight was significantly reduced in $Orai1^{-/-}$ mice, as has previously been reported [22], and changes in reproductive organ weights were proportional to body size.

Histopathological evaluation of the testes of young 8- and 10-week-old mice and mature adult 12–16 week-old mice revealed an essential role for *Orai1* in spermatogenesis. Compared to $Orai1^{+/+}$ testes, spermatid maturation appeared disrupted in 8- and 10-week

old *Orai1*$^{-/-}$ mice (Fig. 6A). Many stage VII seminiferous tubules contained degenerate, clumped and reduced numbers of elongated spermatids (Fig. 6A, arrows), and in some cases there was degeneration and loss of round spermatids (Fig. 6A, arrowhead). In a few of the earlier stage tubules (I, II/III, V, VI) there was vacuolation, exfoliation of spermatocytes and round spermatids, and reduced numbers of elongated spermatids. In tubules between stages IX and XII, there was degeneration and a reduced number of elongated spermatids. In a few tubules, changes were advanced leading to atrophy of the seminiferous tubules (Fig. 6A, bottom right). Leydig cells were unaffected by loss of *Orai1* (not shown). Changes in seminiferous tubules were more advanced in 10-week-old mice (Fig. 6A), and by 12–16 weeks many tubules were atrophic, dilated and contained multinucleated germ cells, sloughed germ cells, abnormal residual bodies and cellular debris (Fig. 7). The cauda epididymis of *Orai1*$^{-/-}$ mice at all ages contained very few sperm and many degenerate cells and cellular debris (Fig. 6B and Fig. 7). These changes were consistent with sperm counts in adult mice (Fig. 5). We conclude that although defects in spermatogenesis can be observed at several stages of development, the major damage to cells occurs late in sperm development, consistent with the finding that the total number of 1n (haploid) cells in the testis is minimally affected (Fig. 2).

Ultrastructural analysis of the testes of adult 12–16 week-old mice confirmed marked defects in spermatogenesis in *Orai1*$^{-/-}$ mice (Fig. 8). Although mild mitochondrial swelling secondary to fixation was observed in both genotypes, diffuse mitochondrial swelling (intracristal and matrical (Fig. 8–iv, MM and ICM)) was observed in *Orai1*$^{-/-}$ mice, as well as abnormalities in junctional complexes (Sertoli-Sertoli, Sertoli-spermatid, and spermatid-spermatid via desmosomes) (Fig. 8-ii, asterisks and 8-vii, S-ES). In addition, some Sertoli cells from *Orai1*$^{-/-}$ mice were observed to have a large, loosely-distended cytoplasm with swollen mitochondria, distended Golgi complexes and an increase in residual bodies, some containing small lipid droplets. Spermatocytes and spermatids from *Orai1*$^{-/-}$ mice also displayed granular, electron lucent nuclear chromatin (Fig. 8-iv, X). However, consistent with the histopathological review, the most striking observation in *Orai1*$^{-/-}$ mice was the near complete loss of elongated spermatids. Rare elongated spermatids that were observed exhibited gross deformations in the sperm head (Fig. 8–iii & 8-v versus 8-iv and 8-vii), although rare cross-sections of the flagella appeared overall normal in these animals (Fig. 8-vi versus 8-viii).

4. DISCUSSION

In this study, we reveal that the Ca^{2+} signal is not only involved in processes important for the normal function of ejaculated sperm [1;23], but that Ca^{2+} signaling via ORAI1 Ca^{2+} channels is essential for sperm development. In a preparation of dispersed testis cells the majority of which were haploid and thus presumably germ cells, all cells from *Orai1*$^{+/+}$ mice but no cells from *Orai1*$^{-/-}$ mice showed store-operated Ca2+ entry in response to thapsigargin (Figs. 2–4). This demonstrates that spermatogenic post-meiotic cells in the testis express functional ORAI1 Ca^{2+} channels which are lost in the *Orai1*$^{-/-}$ mice. Concurrent with this loss of store-operated entry is a marked disruption of sperm development, most obvious at the late stages of development of elongated spermatids (Figs.

6–8). Ultimately, essentially no viable sperm accumulate in the cauda epididymis (Figs. 5–7).

Deletion of calmodulin-dependent protein kinase 4, also results in a failure of spermatogenesis in mice [25]. Previous studies have suggested that store-operated Ca^{2+} channels can contribute to the nature of progesterone-mediated Ca^{2+} signals in human sperm [26], and thus regulate their hyperactivation in the female reproductive tract [27;28]. Indeed, the testis expresses a number of calcium channels, including the testis-specific CATSPER, voltage-dependent Ca^{2+} channels and Ca^{2+}-permeable TRP channels [1]. Of these, only the CATSPER channels have been shown to be required for fertility, but this requirement involves a role in sperm function rather than in sperm development [3]. Here, we reveal a requirement for ORAI1 at a much earlier stage of sperm development, before these cells shed the bulk of their cytoplasm. To our knowledge, the current study represents the first demonstration of a plasmalemmal ion channel requirement for sperm development. While it is possible that the loss of ORAI1 results in endocrine imbalances leading to a failure of spermatogenesis, we consider this unlikely because females are fully fertile, and testis development and mounting behavior appear normal. To our knowledge, no previous studies have identified endocrine imbalances leading to a failure of spermatogenesis at late stages.

An important issue is the signaling pathway that activates ORAI1-dependent Ca^{2+} channels. ORAI1 is a subunit of store-operated channels [29] as well as non-store-operated arachidonic acid-regulated channels [30;31]. Both of these channels are activated downstream of phospholipase C, suggesting a signaling mechanism involving G-protein coupled receptors. Recent studies demonstrated that G-protein coupled tastant receptors and the tastant-coupled G-protein, gustducin, are expressed in the testis [32;33]. In taste buds, sour, sweet and umami tastes are signaled by specific receptors; through the G-protein gustducin, phospholipase C is activated and the ensuing cytoplasmic Ca^{2+} rise initiates the required signaling pathway. Activation of tastant receptors in mouse spermatids increases intracellular calcium [34], and mice lacking the molecular components of this pathway show a failure of sperm development [35]. Further work may determine if the loss of Ca^{2+} entry associated with tastant receptor signaling accounts for the failure of spermatogenesis in ORAI1-deficient mice.

Acknowledgments

We thank John Brodie, Agnes Janoshazi, Page Myers, Pamela Ovwigho, Deloris Sutton and Victor Sutton for technical assistance. We thank Pathology Support Group, Cellular and Molecular Pathology Branch for their help with histology. *Orai1*$^{+/-}$ (*Cracm1*$^{+/-}$) mice were provided by Dr. Jean-Pierre Kinet (Harvard Medical School). We thank Dr. Carl Bortner, in the NIEHS Flow Cytometry Center for his help in sorting and characterizing testicular cell populations. This research was supported by the Intramural Research Program of the National Institutes of Health, National Institute of Environmental Health Sciences.

References

1. Darszon A, Nishigaki T, Beltran C, Trevino CL. Calcium channels in the development, maturation, and function of spermatozoa. Physiol Rev. 2011; 91:1305–1355. [PubMed: 22013213]
2. Publicover S, Harper CV, Barratt C. [Ca2+]i signalling in sperm [mdash] making the most of what you've got. Nat Cell Biol. 2007; 9:235–242. [PubMed: 17330112]

3. Lishko PV, Kirichok Y, Ren D, Navarro B, Chung JJ, Clapham DE. The control of male fertility by spermatozoan ion channels. Annu Rev Physiol. 2012; 74:453–475. [PubMed: 22017176]
4. Avidan N, Tamary H, Dgany O, et al. CATSPER2, a human autosomal nonsyndromic male infertility gene. Eur J Hum Genet. 2003; 11:497–502. [PubMed: 12825070]
5. Hildebrand MS, Avenarius MR, Fellous M, et al. Genetic male infertility and mutation of CATSPER ion channels. Eur J Hum Genet. 2010; 18:1178–1184. [PubMed: 20648059]
6. Avenarius MR, Hildebrand MS, Zhang Y, et al. Human male infertility caused by mutations in the CATSPER1 channel protein. Am J Hum Genet. 2009; 84:505–510. [PubMed: 19344877]
7. Okunade GW, Miller ML, Pyne GJ, et al. Targeted ablation of plasma membrane Ca2+-ATPase (PMCA) 1 and 4 indicates a major housekeeping function for PMCA1 and a critical role in hyperactivated sperm motility and male fertility for PMCA4. J Biol Chem. 2004; 279:33742–33750. [PubMed: 15178683]
8. Miao YL, Williams CJ. Calcium signaling in mammalian egg activation and embryo development: The influence of subcellular localization. Mol Reprod Dev. 2012; 79:742–756. [PubMed: 22888043]
9. Davis FM, Janoshazi A, Janardhan KS, et al. Essential role of Orai1 store-operated calcium channels in lactation. Proc Natl Acad Sci U S A. 2015; 112:5827–5832. [PubMed: 25902527]
10. Miao YL, Stein P, Jefferson WN, Padilla-Banks E, Williams CJ. Calcium influx-mediated signaling is required for complete mouse egg activation. Proc Natl Acad Sci U S A. 2012; 109:4169–4174. [PubMed: 22371584]
11. Feske S, Prakriya M, Rao A, Lewis RS. A severe defect in CRAC Ca2+ channel activation and altered K+ channel gating in T cells from immunodeficient patients. J Exp Med. 2005; 202:651–662. [PubMed: 16147976]
12. Stiber J, Hawkins A, Zhang ZS, et al. STIM1 signalling controls store-operated calcium entry required for development and contractile function in skeletal muscle. Nat Cell Biol. 2008; 10:688–697. [PubMed: 18488020]
13. Xing J, Petranka JG, Davis FM, Desai PN, Putney JW, Bird GS. Role of orai1 and store-operated calcium entry in mouse lacrimal gland signaling and function. J Physiol (Lond). 2013; 592:927–939. [PubMed: 24297846]
14. Davis FM, Parsonage MT, Cabot PJ, et al. Assessment of gene expression of intracellular calcium channels, pumps and exchangers with epidermal growth factor-induced epithelial-mesenchymal transition in a breast cancer cell line. Cancer Cell Int. 2013; 13:76. [PubMed: 23890218]
15. Suchanek KM, May FJ, Robinson JA, et al. Peroxisome proliferator-activated receptor alpha in the human breast cancer cell lines MCF-7 and MDA-MB-231. Mol Carcinog. 2002; 34:165–171. [PubMed: 12203367]
16. O'Brien, DA. Isolation, separation and short-term culture of spermatogenic cells. In: Chapin, RE.; Heindel, JJ., editors. Methods in Toxicology. San Diego, CA: Academic Press; 1993. p. 246-264.
17. Lasalle B, Bastos H, Louis JP. "Side Population" cells in adult mouse testis express Brcp1 gene and are enriched in spermatagonia and germinal stem cells. Development. 2004; 131:479–487. [PubMed: 14681185]
18. Bird GS, Putney JW. Capacitative calcium entry supports calcium oscillations in human embryonic kidney cells. J Physiol. 2005; 562:697–706. [PubMed: 15513935]
19. Feske S. CRAC channelopathies. Pflugers Arch. 2010
20. Janca FC, Jost LK, Evenson DP. Mouse testicular and sperm cell development characterized from birth to adulthood by dual parameter flow cytometry. Biol Reprod. 1986; 34:613–623. [PubMed: 3708046]
21. Bird GS, DeHaven WI, Smyth JT, Putney JW Jr. Methods for studying store-operated calcium entry. Methods. 2008; 46:204–212. [PubMed: 18929662]
22. Vig M, DeHaven WI, Bird GS, et al. Defective mast cell effector functions in mice lacking the CRACM1 pore subunit of store-operated calcium release-activated calcium channels. Nat Immunol. 2008; 9:89–96. [PubMed: 18059270]
23. Chung JJ, Navarro B, Krapivinsky G, Krapivinsky L, Clapham DE. A novel gene required for male fertility and functional CATSPER channel formation in spermatozoa. Nat Commun. 2011; 2:153. [PubMed: 21224844]

24. Braun RE, Behringer RR, Peschon JJ, Brinster RL, Palmiter RD. Genetically haploid spermatids are phenotypically diploid. Nature. 1989; 337:373–376. [PubMed: 2911388]
25. Wu JY, Ribar TJ, Cummings DE, Burton KA, McKnight GS, Means AR. Spermiogenesis and exchange of basic nuclear proteins are impaired in male germ cells lacking Camk4. Nat Genet. 2000; 25:448–452. [PubMed: 10932193]
26. Blackmore PF. Thapsigargin elevates and potentiates the ability of progesterone to increase intracellular free calcium in human sperm: Possible role of perinuclear calcium. Cell Calcium. 1993; 14:53–60. [PubMed: 8382564]
27. Lefievre L, Nash K, Mansell S, et al. 2-APB-potentiated channels amplify CatSper-induced Ca(2+) signals in human sperm. Biochem J. 2012; 448:189–200. [PubMed: 22943284]
28. Morris J, Jones S, Howl J, Lukanowska M, Lefievre L, Publicover S. Cell-penetrating peptides, targeting the regulation of store-operated channels, slow decay of the progesterone-induced [Ca2+]i signal in human sperm. Mol Hum Reprod. 2015; 21:563–570. [PubMed: 25882543]
29. Hogan PG, Lewis RS, Rao A. Molecular basis of calcium signaling in lymphocytes: STIM and ORAI. Annu Rev Immunol. 2010; 28:491–533. [PubMed: 20307213]
30. Shuttleworth TJ, Thompson JL, Mignen O. STIM1 and the noncapacitative ARC channels. Cell Calcium. 2007; 42:183–191. [PubMed: 17391754]
31. Zhang X, Gonzalez-Cobos JC, Schindl R, et al. Mechanisms of STIM1 activation of store-independent leukotriene C4-regulated Ca2+ channels. Mol Cell Biol. 2013; 33:3715–3723. [PubMed: 23878392]
32. Li F, Zhou M. Depletion of bitter taste transduction leads to massive spermatid loss in transgenic mice. Mol Hum Reprod. 2012; 18:289–297. [PubMed: 22266327]
33. Li F. Taste perception: from the tongue to the testis. Molecular Human Reproduction. 2013; 19:349–360. [PubMed: 23423265]
34. Xu J, Cao J, Iguchi N, Riethmacher D, Huang L. Functional characterization of bitter-taste receptors expressed in mammalian testis. Mol Hum Reprod. 2013; 19:17–28. [PubMed: 22983952]
35. Mosinger B, Redding KM, Parker MR, et al. Genetic loss or pharmacological blockade of testes-expressed taste genes causes male sterility. Proc Natl Acad Sci U S A. 2013; 110:12319–12324. [PubMed: 23818598]

Highlights

- Orai1 knockout male mice are sterile.
- Mouse testicular cells, including germ cells, have robust store-operated calcium entry, and this is completely lost in Orai1 knockout mice.
- In the testes of Orai1 knockout mice, mature sperm fail to develop fully or survive.
- Orai1-mediated Ca^{2+} entry appears necessary for the late stages of sperm development.

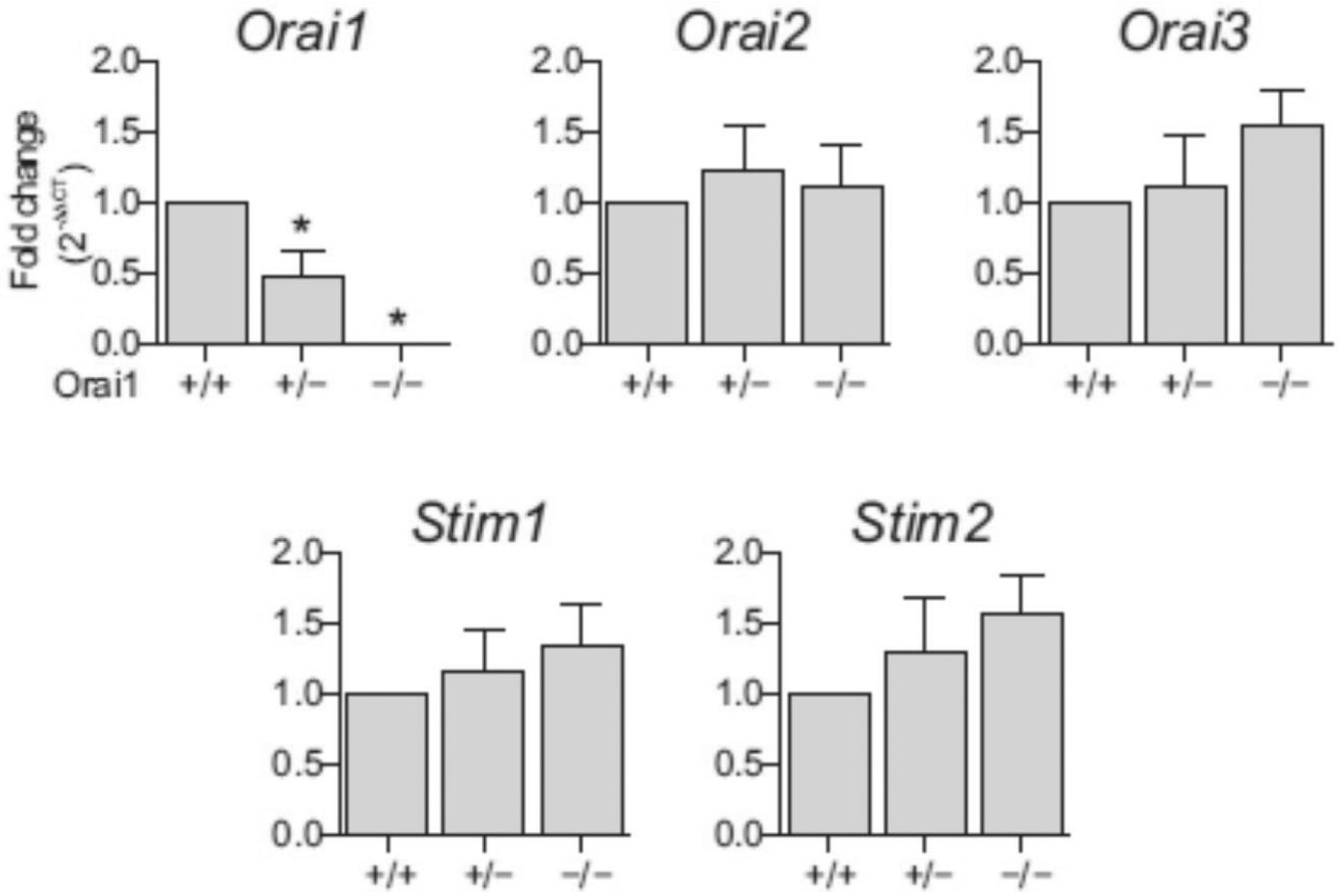

Fig. 1.

Comparative expression of *Orai* and *Stim* message forms in the mouse. Relative mRNA levels of *Orai1*, *Orai2*, *Orai3*, *Stim1* and *Stim2* in testes of $Orai1^{+/+}$, $Orai1^{+/-}$ and $Orai1^{-/-}$ mice.

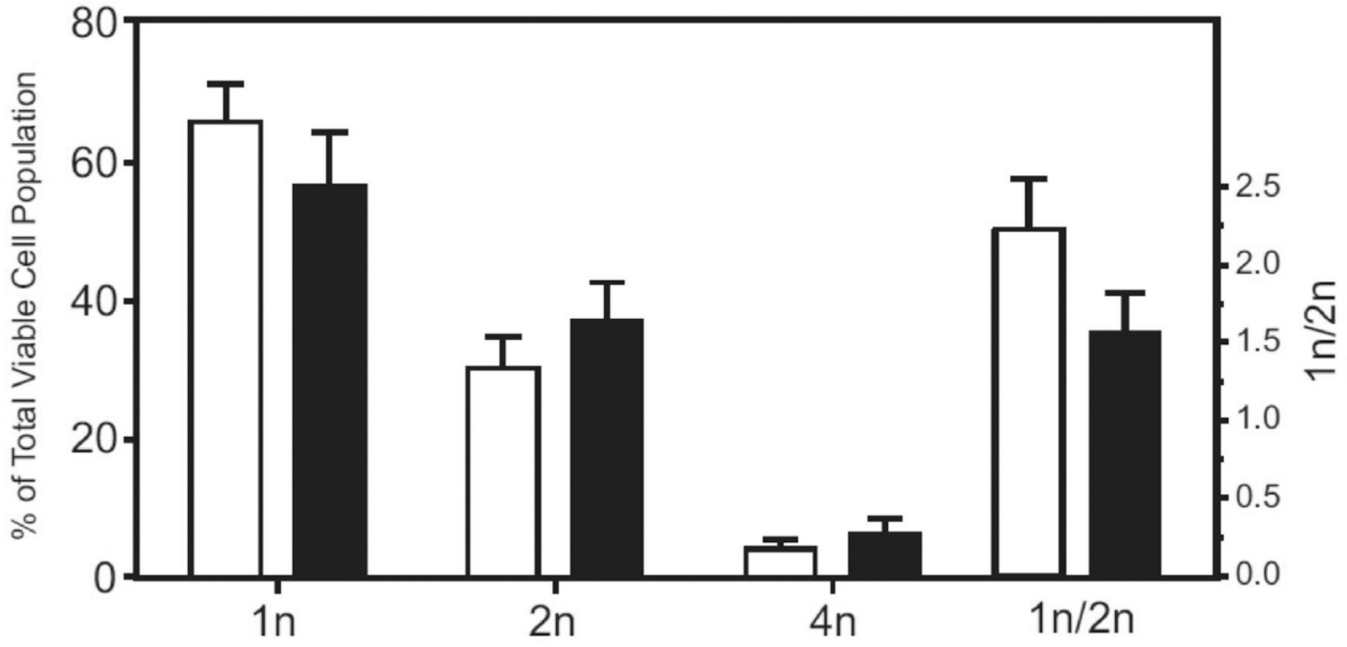

Fig. 2.

Flow cytometric analysis of Hoechst 33342 fluorescence in *Orai1*$^{+/+}$ (open bars) and *Orai1*$^{-/-}$ (filled bars) mouse testis cells. Single cell populations of mouse testis stained with Hoechst 33342 were analyzed by flow cytometry. An analysis using forward-scatter versus Hoechst Blue (Ex. 405 nm, Em. 440/40) and Hoechst Red (Ex. 405 nm; Em. 605/40) versus Hoechst Blue was employed to classify cell populations as 1n, 2n or 4n. The data are mean ± SEM from 3 independent experiments, with at least 45,000 viable cells sorted per experiment.

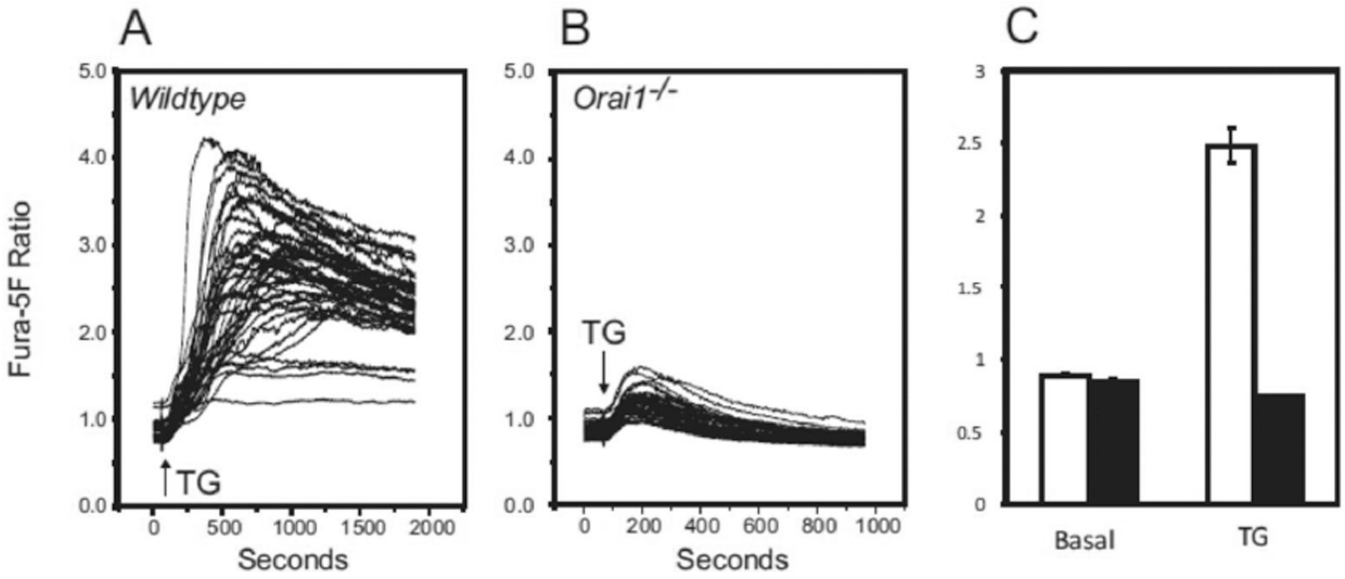

Fig. 3.

Characterization of the $[Ca^{2+}]_i$ signaling response to thapsigargin in mouse testis cells loaded with the calcium sensitive dye fura-5F. Mouse testis cells isolated from (A) *Orai1*$^{+/+}$ and (B) *Orai1*$^{-/-}$ mice were loaded with fura-5F and treated with thapsigargin (TG) in HBSS containing 1.8 mM extracellular calcium. A and B: Ensemble $[Ca^{2+}]_i$ ratio responses to TG added at t = 60 sec (42 – 48 cells in the field). B: C: Comparison of basal $[Ca^{2+}]_i$ ratio levels (measured at t = 40 sec) and TG-induced $[Ca^{2+}]_i$ ratio (measured at t = 960 sec) in *Orai1*$^{+/+}$ (open bars) and *Orai1*$^{-/-}$ (filled bars) testis cells; data are mean ± SEM from 3 independent experiments.

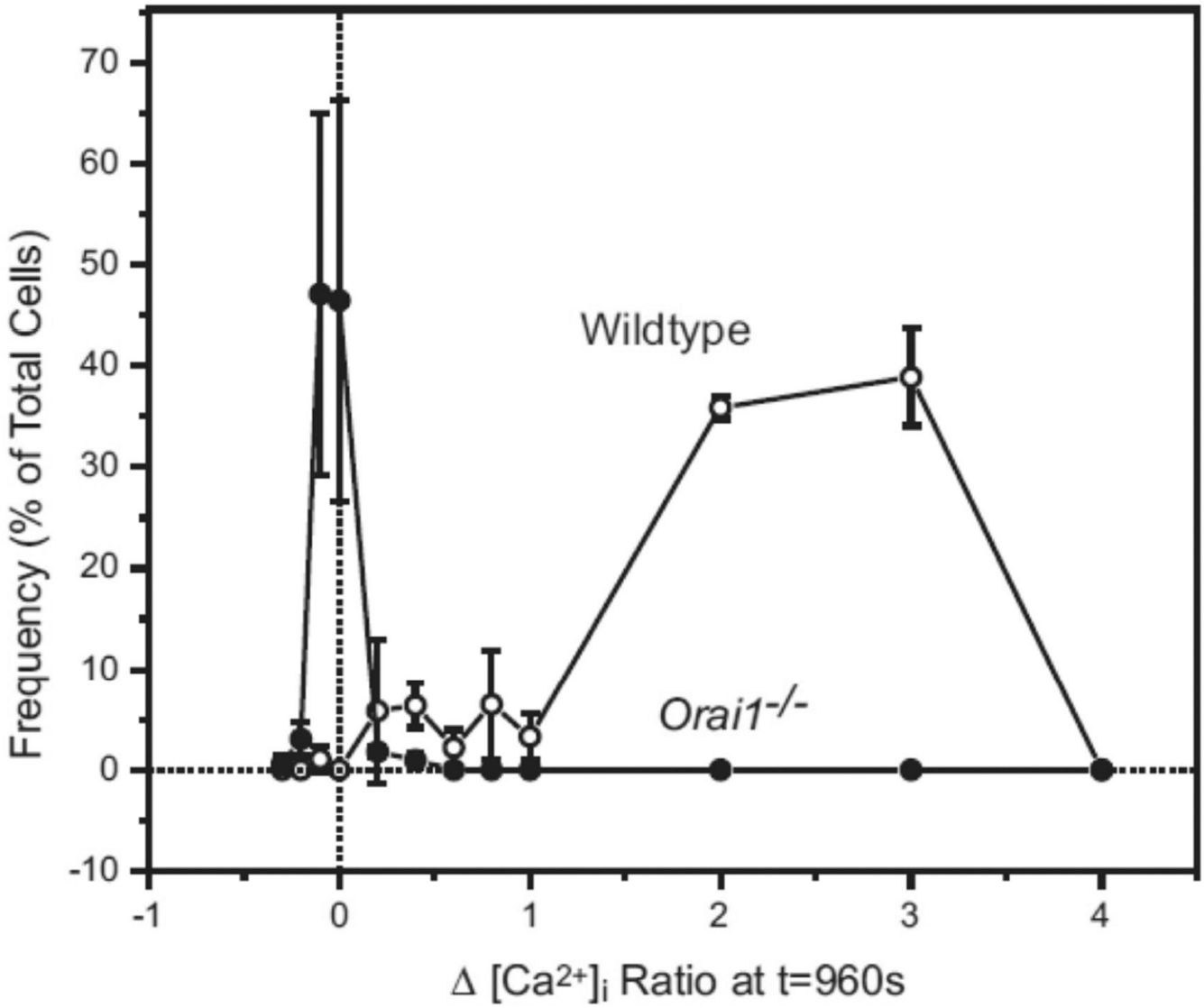

Fig. 4.

Frequency plot comparing the thapsigargin–induced $[Ca^{2+}]_i$ signaling response in *Orai1*$^{+/+}$ and Orai1-KO testis cells loaded with the calcium sensitive dye fura-5F. Using the $[Ca^{2+}]_i$ ratio data reported in figure 3, the TG–induced $[Ca^{2+}]_i$ response (at t = 960 sec) in each individual cell was measured against basal levels measured before TG treatment. The resulting $\Delta[Ca^{2+}]_i$ Ratios for *Orai1*$^{+/+}$ (○) and *Orai1*$^{-/-}$ cells (●) is represented as a frequency plot; data are mean ± SEM from 3 independent experiments.

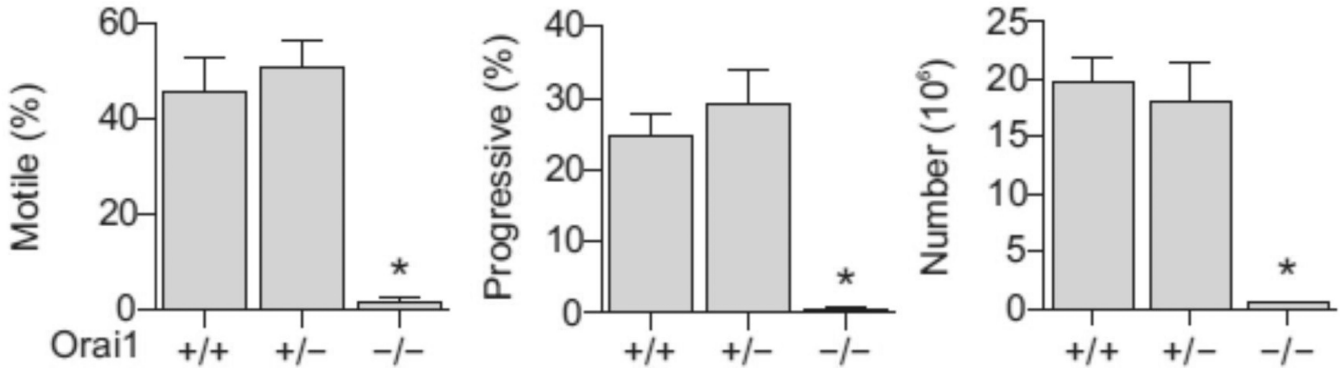

Fig. 5.

Sperm analyses in testes from *Orai1*$^{+/+}$, *Orai1*$^{+/-}$ and *Orai1*$^{-/-}$ mice. Sperm motility, progressive motility and total number in samples extracted from the cauda epididymis of mature adult *Orai1*$^{+/+}$, *Orai1*$^{+/-}$ and *Orai1*$^{-/-}$ mice. Means ± SEM (n = 3), $P < 0.05$, one-way ANOVA with Bonferroni post-tests.

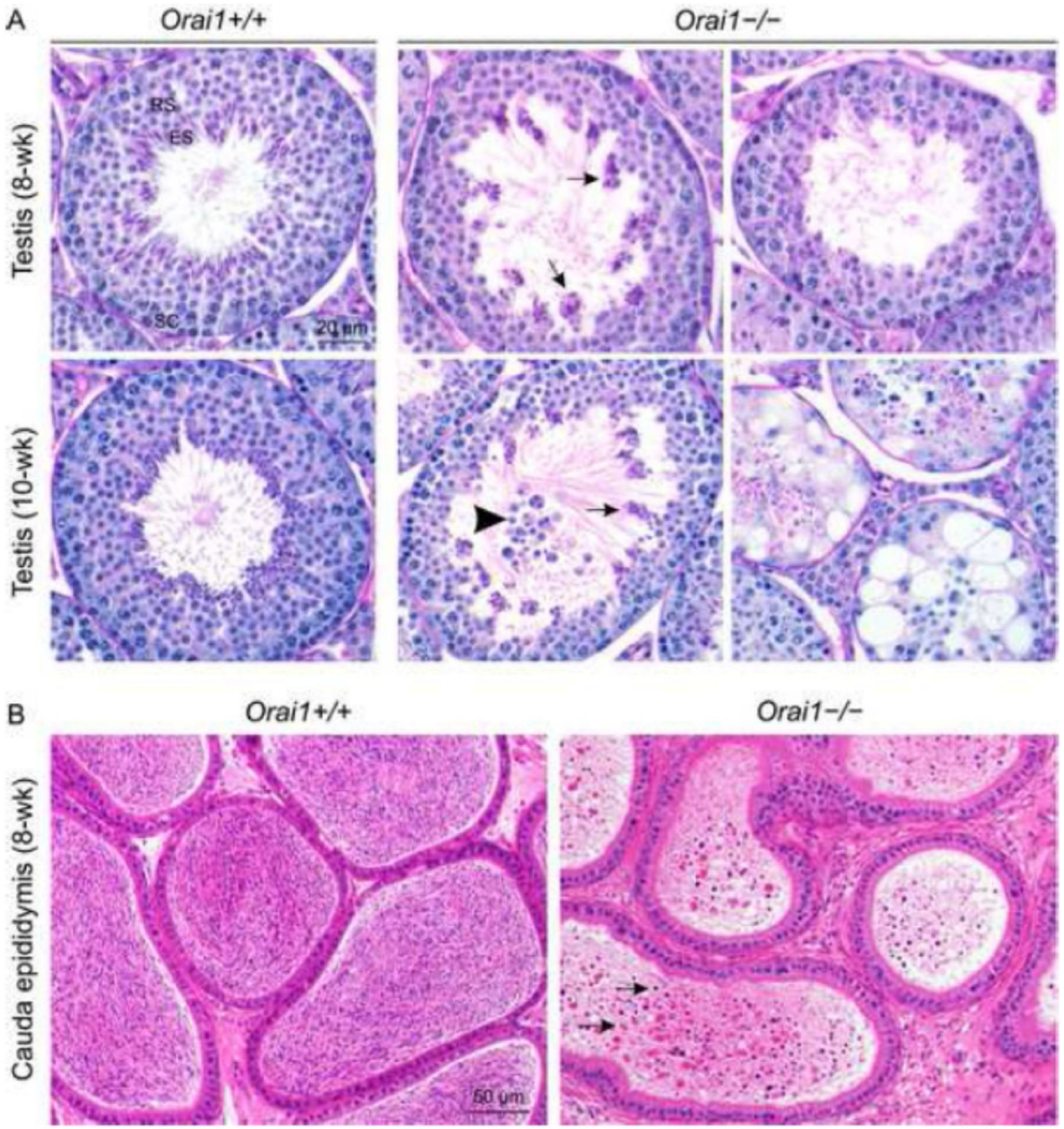

Fig. 6.

Histopathological analysis of the testis and cauda epididymis of *Orai1*$^{-/-}$ mice. A, Stage VII seminiferous tubules from 8- and 10-week-old *Orai1*$^{+/+}$ mice with elongated spermatids lining the lumen of the seminiferous tubule (Periodic Acid Schiff-Hematoxylin staining; RS, round spermatids; ES elongated spermatids; SC, spermatocytes) versus *Orai1*$^{-/-}$ mice with numerous poorly populated seminiferous tubules. Arrows: degenerate and clumped elongated spermatids. Arrowhead: exfoliation of round spermatids. B, Hematoxylin and eosin staining of the cauda epididymis from 8-week-old *Orai1*$^{-/-}$ versus *Orai1*$^{+/+}$ mice. The

cauda epididymis in WT mice is full of normal sperm, whilst that of *Orai1*$^{-/-}$ mice contains very low number of sperm admixed with cellular debris (arrows). For 8-week-old samples (n = 3 mice/group) and for 10-week-old samples (n = 2 mice/group).

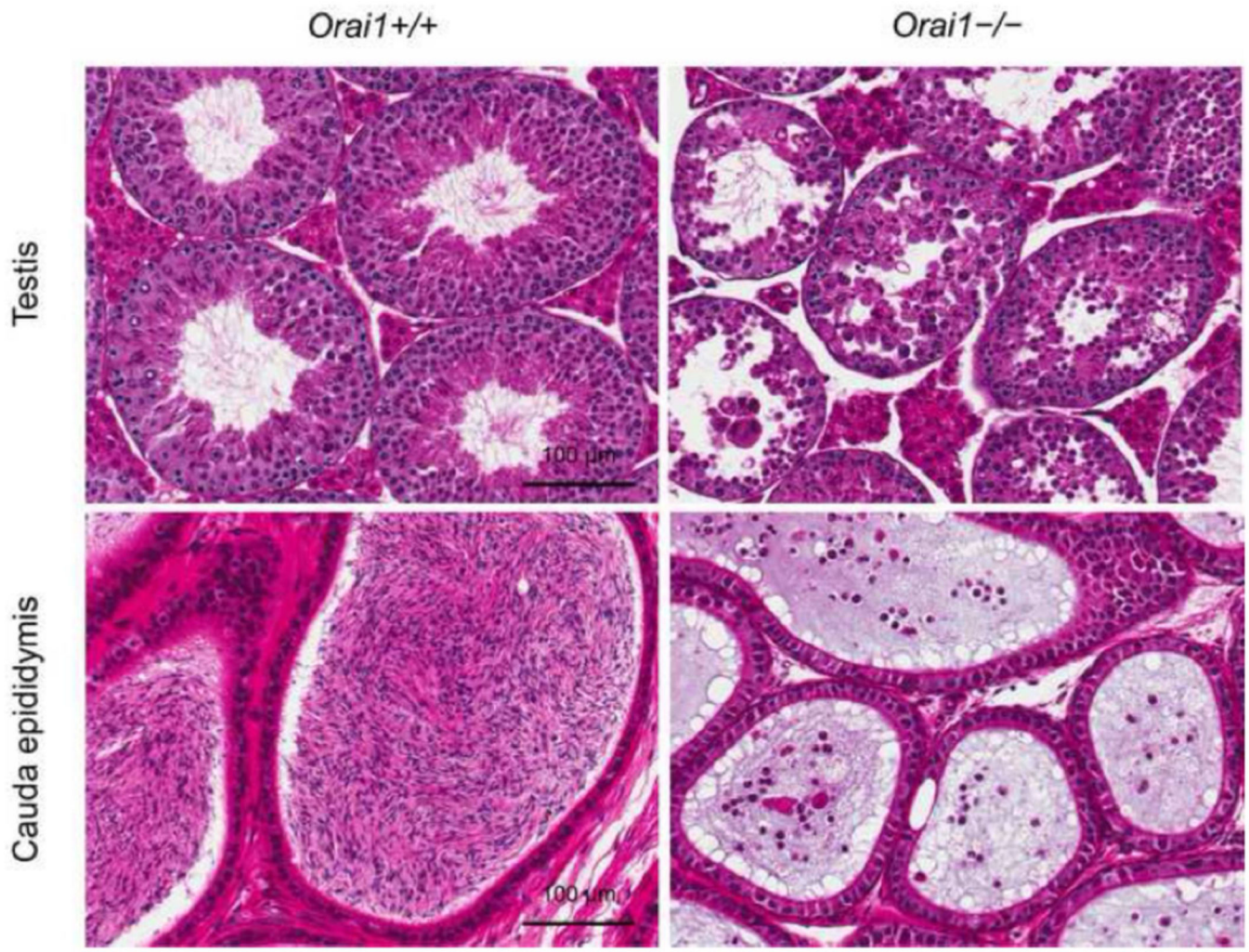

Fig. 7.

Histopathological analyses of the reproductive organs of mature adult *Orai1*$^{+/+}$ and *Orai1*$^{-/-}$ mice. Seminiferous tubule and cauda epididymis sections of adult (12–16-week-old) *Orai1*$^{+/+}$ and *Orai1*$^{-/-}$ mice stained with H&E. Compared to *Orai1*$^{+/+}$, there is seminiferous tubule atrophy along with degeneration and loss of spermatocytes and spermatids in the *Orai1*$^{-/-}$ mouse. Changes in the testes are reflected in cauda epididymis with the *Orai1*$^{+/+}$ mouse containing normal sperm and *Orai1*$^{-/-}$ mouse containing only the cellular debris (n = 3 mice/group).

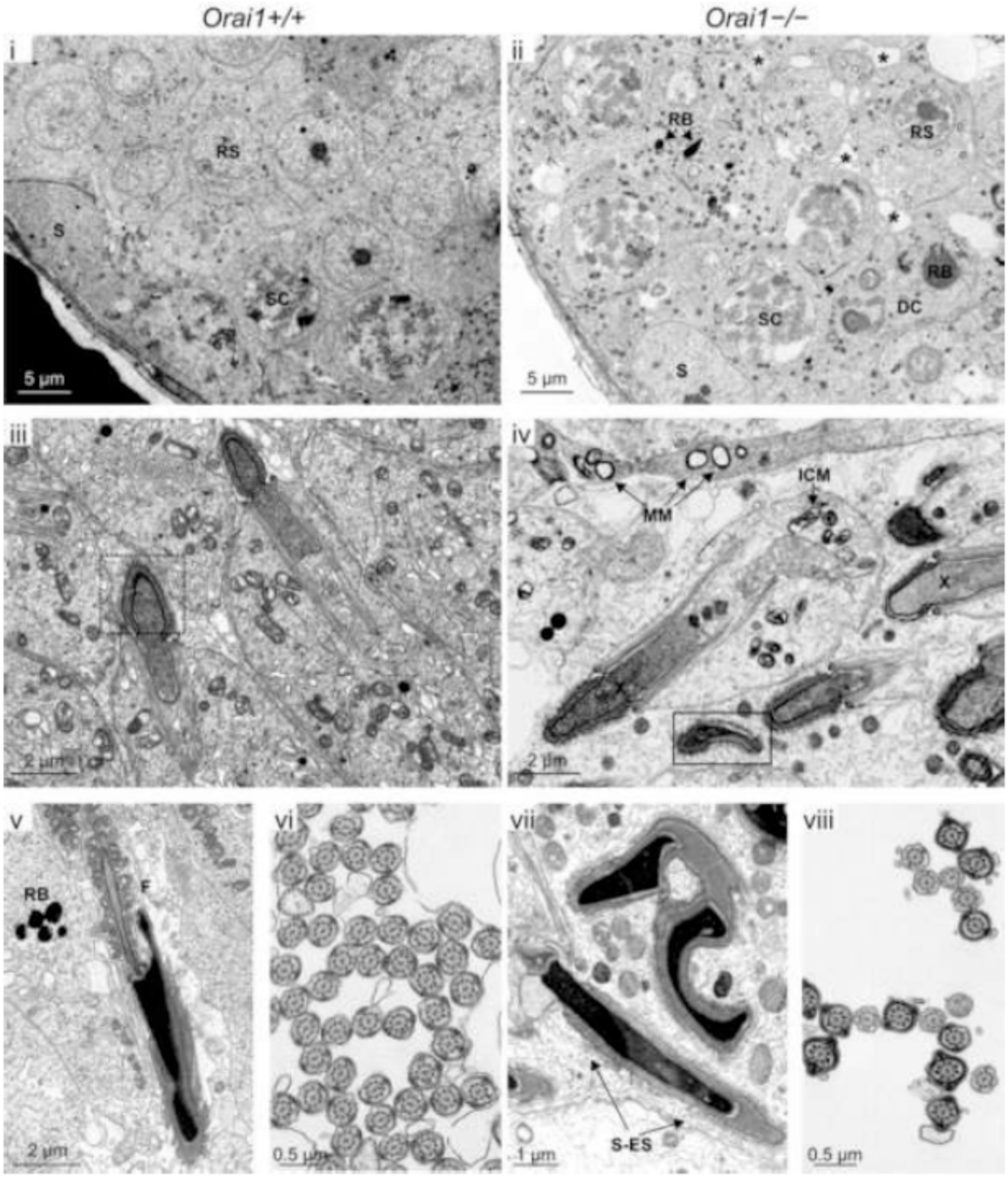

Fig 8.

Ultrastructural analysis of randomly selected seminiferous tubules within the testis of *Orai1*$^{+/+}$ and *Orai1*$^{-/-}$ mice. Digital transmission electron photomicrographs of seminiferous tubules from *Orai1*$^{+/+}$ and *Orai1*$^{-/-}$ mice were compared. Individual letters on each image identify the particular structure: DC, degenerating cell; F, flagella; ICM, intracristal mitochondrial swelling; MM, matrical mitochondrial swelling; RB, residual body; RS, round spermatid, S, Sertoli cell; SC, spermatocyte; and S-ES, Sertoli-elongating spermatid junction. Small asterisks in (ii) show swelling of the junctional complexes between

spermatids and/or Sertoli and spermatids, whereas swelling along the junctional complexes were sparse in the *Orai1*$^{+/+}$ tubules (i). Dashed box in (iii) shows a normal spermatid head at early elongating stage versus in the solid box (iv), early elongating spermatids had an abnormal head and loosely stippled to granular nuclear material (X). n = 3 mice/group. Lastly, when observed, distinct ultrastructural defects in later elongating stages included extensive malformations of the sperm head. (Fig. 7–iv, 7vii, 7-viii). Moreover, cross-sections of the flagella from a *Orai1*$^{+/+}$ and *Orai1*$^{-/-}$ mouse when compared showed mostly normal formation; however, there was clearly a difference between the numbers of flagella in cross section from an *Orai1*$^{+/+}$mice compared with *Orai1*$^{-/-}$ mice, the latter having a marked decrease in the number of cross-sectional flagella (Fig. 7–vi versus 7-viii).

Table 1

Fertility of adult (12–16-wk-old) males determined by rotated matings for two months with wildtype females

Orai1 genotype	No. of males mated	No. of litters produced	% Fertile
+/+	3	12	100
−/−	3	0	0

Table 2

Reproductive organ weights

Orai1 genotype	Testis, g	Cauda epididymis, g	Seminal vesicle, g	Body weight, g
+/+	0.131 ± 0.007	0.020 ± 0.001	0.305 ± 0.021	36.50 ± 2.669
+/−	0.144 ± 0.008	0.019 ± 0.002	0.342 ± 0.040	39.37 ± 2.800
−/−	0.085 ± 0.014 *	0.014 ± 0.001	0.232 ± 0.028	24.07 ± 1.650 *

Adult male mice (12–16 weeks) were sacrificed and reproductive organ and total body weights were recorded. Values show mean ± s.e.m. from 3 animals of each genotype.

* $P < 0.05$, One-way ANOVA with Bonferroni post-tests.